

Cite this: *Dalton Trans.*, 2017, **46**, 16474

Topological transformation of a trefoil knot into a [2]catenane†

Thirumurugan Prakasam,^a Rana A. Bilbeisi,^b Roberto El-Khoury,^a Loïc J. Charbonnière,^c Mourad Elhabiri,^d Gennaro Esposito,^e John-Carl Olsen^f and Ali Trabolsi^{*,a}

Topological transformation of a zinc-templated trefoil knot, **Zn-TK**, into a zinc-templated [2]catenane, **Zn-[2]C**, was studied. The net reaction $2 \text{ Zn-TK} \rightarrow 3 \text{ Zn-[2]C}$ was accomplished in 89% yield by heating a solution of **Zn-TK** in D₂O. Kinetic investigation by ¹H NMR spectroscopy and high resolution mass spectrometry revealed that the mechanism is complex, involving a large pool of intermediates that form after imine bond cleavage. Bromide ions, which can occupy the central cavity of **Zn-TK**, inhibited the reaction. Two similar transformations were also studied, one of a cadmium-containing trefoil knot, **Cd-TK**, into a cadmium-containing catenane, **Cd-[2]C**, and the other of **Cd-TK** into **Zn-[2]C**. The latter transformation could be achieved in one step at high temperature or in two steps *via* transmetalation to form **Zn-TK** at room temperature followed by topological conversion of **Zn-TK** to **Zn-[2]C** at high temperature.

Received 22nd September 2017.

Accepted 23rd October 2017

DOI: 10.1039/c7dt03582a

rsc.li/dalton

During the past several decades, reliable principles for the rational design of discrete metal-organic coordination complexes have been devised and applied.¹ The study of isolated complexes and the investigation of their structural interconversions² are now leading to the development of more refined guidelines for structural design,³ as well as a deeper understanding of dynamic metallo-supramolecular systems. Regarding systems, reports have described conversions between triangles and squares,⁴ rhomboids and hexagons,⁵ small prisms and large prisms,⁶ helicates and grids,⁷ or bis-rhombuses and tetrahedrons,⁸ to name a few, and these studies have elucidated the effects that changes in, for example, cation,⁷ anion,⁹ solvent,¹⁰ complex concentration,⁸ sub-component ratios,¹¹ or that external stimuli such as light¹² or heat,¹³ have on the equilibria of the corresponding reactions.

Previously, we reported a one-pot synthesis of three topologically non-trivial zinc-based complexes: a [2]catenane (**Zn-2[C]**), a trefoil knot (**Zn-TK**), and a Solomon link (**Zn-SL**).^{14,15} The complexes formed spontaneously when equimolar amounts of the organic ligands diamino-2,2'-bipyridine (DAB) and diformylpyridine (DFP) were combined with zinc triflate in a ternary 1:1:1 solvent mixture of D₂O, MeOD, and CD₃CN.¹⁵ Alternatively, when the ligands were mixed with zinc acetate in 1:1, D₂O:MeOD, only **Zn-2[C]** and **Zn-TK** were formed. The mole ratio of the two complexes were monitored in solution at different reaction temperatures ranging from 50 °C to 90 °C. When the temperature was 50 °C, **Zn-TK** was the major product (by a ratio of 63 to 37), whereas, at 90 °C, **Zn-2[C]** formed exclusively. From these results, we inferred that a direct topological transformation from **Zn-TK**¹⁶ to **Zn-2[C]** might be achieved at a sufficiently high temperature.

We now report that this conversion is possible and provide a detailed kinetic analysis of the process by NMR spectroscopy and high resolution mass spectrometry (HRMS). The former allowed us to determine activation parameters, and the latter lead to the identification of a large pool of intermediates. We also found that bromide ion inhibits the reaction by stabilizing the knot. Also, the transformation of the analogous cadmium (II)-containing trefoil knot **Cd-TK** to either **Cd-2[C]** or **Zn-2[C]** was achieved at elevated temperature in aqueous solution.

The **Cd-TK** to **Zn-2[C]** reaction involved heating a solution of **Cd-TK** to 90 °C in the presence of zinc(II) acetate. Alternatively, transmetalation of **Cd-TK** to **Zn-TK** could be realized first at room temperature and followed by conversion

^aNew York University Abu Dhabi (NYUAD), Experimental Research Building, Building C1, Saadiyat Island, Abu Dhabi, United Arab Emirates.
E-mail: ali.trabolsi@nyu.edu

^bAmerican University of Beirut, Department of Civil and Environmental Engineering (CEE), Faculty of Engineering and Architecture (FEA), Beirut, Lebanon

^cLaboratoire d'Ingénierie Moléculaire Appliquée à l'Analyse, IPHC UMR 7178 CNRS-Université de Strasbourg, ECPM, 25 rue Becquerel, 67087 Strasbourg, France

^dLaboratoire de Chimie Bioorganique et Médicinale, UMR 7509 CNRS-Université de Strasbourg, ECPM, 25 rue Becquerel, 67087 Strasbourg, France

^eDMIE, Udine University, 33100 Udine, Italy

^fDepartment of Chemistry, RC Box 270216, University of Rochester, Rochester, NY, 14627, USA

† Electronic supplementary information (ESI) available: Additional characterization of all topological transformations. See DOI: 10.1039/c7dt03582a

to Zn-[2]C at higher temperature. These transformations are among a very few reported¹⁷ that involve conversion between topologically non-trivial¹⁸ metal-organic architectures.

Results and discussion

Heat-induced transformation of Zn-TK into Zn-[2]C

A preliminary experiment analyzed by ¹H NMR spectroscopy first demonstrated that heating an aqueous solution of pure Zn-TK (Fig. 1, *t* = 0 h) gradually converts the knot to Zn-[2]C. A 1.7 mM D₂O solution of Zn-TK was placed in a NMR tube and heated to 90 °C. The progress of the reaction was monitored by brief ¹H NMR measurements at room temperature. Over time, new sets of highly symmetric peaks appeared that were merged with or grew adjacent to shrinking peaks that corresponded Zn-TK.

After 70 h (Fig. 1), the signals corresponding to Zn-TK had almost completely disappeared, while the set of signals corresponding to Zn-[2]C had become prominent. The catenane was further characterized by HRMS which showed two *m/z* maxima at 704.1375 and 431.7696 that correspond to (Zn-[2]C·2CF₃COO⁻)²⁺ and (Zn-[2]C·CF₃COO⁻)³⁺, respectively. Thus, both NMR and HRMS results provided clear evidence for the formation of Zn-[2]C from Zn-TK.

The conversion was then monitored in more spectroscopic detail. Four solutions of Zn-TK in D₂O (1.7 mM) were heated to different temperatures (50, 60, 70 or 80 °C), and ¹H NMR spectra of each sample were acquired at regular time intervals (Fig. 2). The *h* and *j* protons (Fig. 1) of Zn-TK and Zn-[2]C were

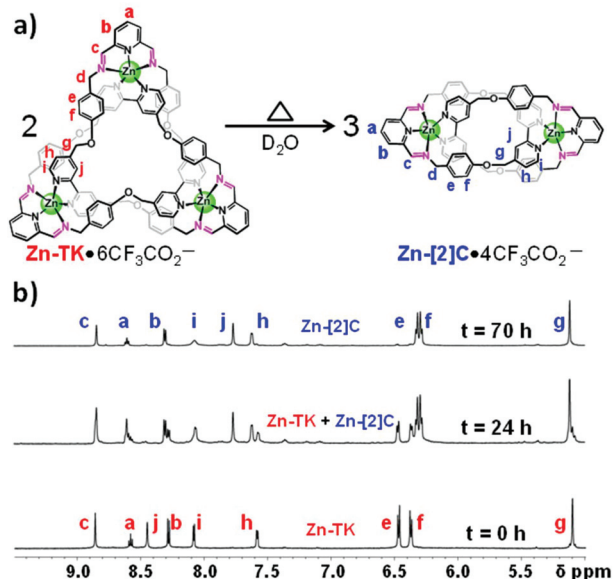


Fig. 1 (a) Schematic representation of the temperature-induced conversion of Zn-TK·6CF₃COO⁻ into Zn-[2]C·4CF₃COO⁻. (b) Aromatic regions of ¹H NMR spectra of a 1.7 mM solution of Zn-TK in D₂O after 0 h (bottom), 24 h (middle) and 70 h (top) of heating at 90 °C. Peaks that correspond to Zn-[2]C are apparent after 24 h and are nearly the only ones remaining after 70 h.

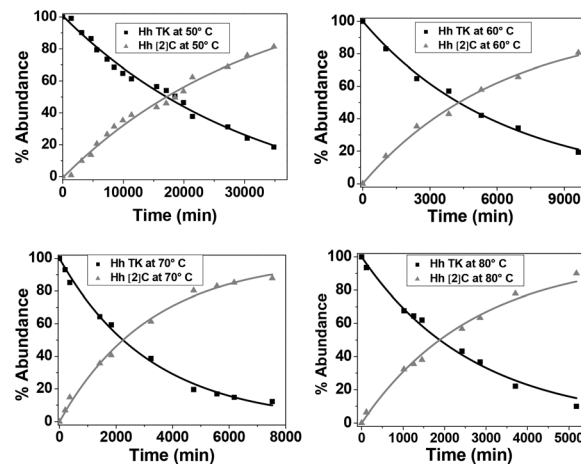


Fig. 2 Relative abundance of Zn-TK (black squares) and Zn-[2]C (grey triangles) plotted against reaction time. Solutions of Zn-TK (1.7 mM) in D₂O were heated to four different temperatures (50, 60, 70 or 80 °C). Integration of the H_h proton NMR signals arising from Zn-TK and Zn-[2]C were used to determine mole percentages. (See Fig. 1 for proton assignment.)

monitored as Zn-TK was consumed and Zn-[2]C produced. The signal intensities of these protons, which define the starting materials and final products, varied over substantial time intervals in a nearly mono-exponential fashion (Fig. 2). For a conceivably complex mechanism involving the non-trivial conversion herein described, this exponential trend clearly suggested the presence of a dominant rate limiting step. At this stage, hypothesizing preceding or following steps, that escape NMR kinetic characterization because of the lack of observable signals from the intervening intermediates, does not provide any valuable insight without knowing the exact nature of the rate determining step and the subsequent set of species involved.

With the assumption that the transformation involves a single rate-limiting step that corresponds to the observed apparent first order rate constant *k*₁ (s⁻¹) and assuming that *k*₁ ≫ *k*₋₁ (Fig. S11a†), the kinetic evolutions were fitted to extract the *k*_{obs} values at the different temperatures (Fig. S2–S7†). Furthermore, different starting concentrations of Zn-TK (0.85, 1.7 and 3.4 mM) were evaluated as a function of temperature (Fig. S1–S7†). From these sets of kinetic data, Arrhenius plots were constructed and an estimate of the apparent activation energy of the process, *E*_a, of 79 ± 9 kJ mol⁻¹ was calculated. Furthermore, HRMS analysis of the reaction indicated the presence of a pool of intermediates (Fig. S9 and S10†).

In order to study the involvement of intermediates, we carried out the reaction at constant temperatures, in the range of 50–90 °C, inside the NMR magnet for 120 hours. Typically, a D₂O solution of Zn-TK (0.6 mL and 1.7 mM) was placed in a NMR tube inside the magnet, and maintained at a fixed temperature while 2D arrays of 400 proton spectra were collected at 18.75 minutes intervals. Unfortunately, the overlap of many signals corresponding to Zn-TK and Zn-[2]C and the absence of any resolved signals associated with reaction intermediates prevented quantification of these species. A complete kinetic

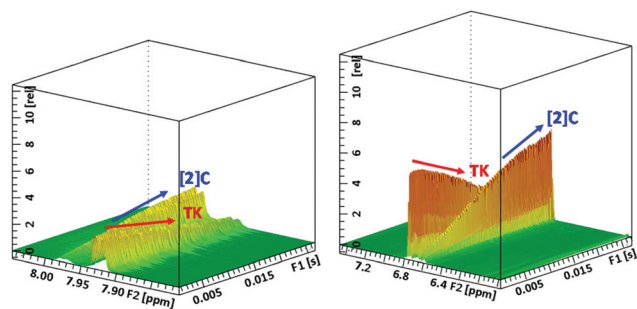


Fig. 3 3D stacked ^1H NMR spectra showing h (left cube) and e and f (right cube) proton signals corresponding to **Zn-TK** (indicated by red arrows) and **Zn-[2]C** (indicated by blue arrows). At 90°C in D_2O , signals corresponding to protons in **Zn-TK** decrease in intensity, while signals corresponding to **Zn-[2]C** increase in intensity. F2 axes: chemical shift in ppm. F1 axes: time in seconds. Z axes: intensity.

analysis and a detailed elucidation of the reaction's mechanism were therefore not possible.

In this second set of experiments, we were able to rely on only a single well resolved resonance from **Zn-[2]C**, namely from proton h , and a single well resolved resonance from **Zn-TK**, namely from proton e (Fig. 3). During the progress of the reaction, the changes in the intensities of these peaks tracked the formation of **Zn-[2]C** and the consumption of **Zn-TK** and indicated a complex kinetic process involving steady-state equilibria between the **Zn-TK** starting material and a pool of intermediates and between those intermediates and the **Zn-[2]C** product (Fig. S11a†). These kinetic inferences derive from an analysis using only single exponential fitting of the initial kinetic data. From this assessment, an overall scenario emerges involving a number of intermediates whose steady state populations cannot be analyzed without sampling specific corresponding signals.

Thermodynamic analysis

Thermodynamic parameters (ΔH° and ΔS°) of supramolecular equilibria are rarely been measured and reported.^{19a,b} To the best of our knowledge, such analysis has never been applied to molecular knots and links until now. The data that were herein acquired to determine the kinetics parameters could also be used to extract the relevant thermodynamic parameters of the considered reaction. For this purpose and since proper

temperature control was possible only for the samples heated in the NMR magnet, we decided to use the signal integrals of the last-recorded trace of each 2D array. Because of the very slow rate of the process we observed under NMR probe conditions, reaching the complete conversion equilibrium was not feasible in terms of spectrometer time. Hence we choose to assess an operative parameter by calculating the same law of mass action quotient used for equilibrium constant after more than 120 hours at constant temperature. We could thus estimate an apparent constant at different temperatures for the direct transformation process of **TK** into **[2]C** and thereby perform an approximate thermodynamic analysis. Since the individual 1D spectra of the pseudo 2D experiment were collected with a short recycling time between successive scans (overall 1.22 s), to minimize systematic errors from possible relaxation rate differences, we used NMR signals from the same corresponding positions within the two species, namely those of the two corresponding h nuclei that remain slightly merged and do not coalesce even at 363 K in the Zn analogues. We applied a deconvolution algorithm to estimate the relative percentage resonance areas of the individual species. Those areas correspond to the respective mole fractions of **TK** and **[2]C** and were exploited to calculate the apparent equilibrium constant at each temperature and the ΔG° values and to finally perform a van't Hoff analysis according to:

$$K = \frac{[[2]C]^3}{[TK]^2} \quad \text{and} \quad \ln K = -\frac{\Delta G^\circ}{RT} = -\frac{\Delta H^\circ}{RT} + \frac{\Delta S^\circ}{R}$$

The relevant data are reported in Table 1. The apparent enthalpy of interconversion of **Zn-TK** into **Zn-[2]C** is positive ($\Delta H^\circ = 106 \text{ kJ mol}^{-1}$, see ESI Fig. 8a†) accounting for the stability of **Zn-TK** with respect to the product over a substantial temperature interval. The corresponding entropic contribution is quite large and positive ($\Delta S^\circ = 247 \text{ J mol}^{-1} \text{ K}^{-1}$, see ESI Fig. 8a†) as expected for reactions entailing an increase of molecular units. A further control was performed to estimate the reliability of the apparent constant error. The parameter was evaluated at 55°C using three different starting product concentrations (0.85, 1.7 and 3.4 mM) and the obtained value showed a maximum deviation of 10% around the average. This uncertainty was considered to represent the limiting error when it proved larger than the deviation calculated from the individual signal area assessments. The thermodynamic

Table 1 Thermodynamic parameters for the **Zn-[2]C/Zn-TK** equilibrium in D_2O

Temperature (K)	%(Zn-TK)	%(Zn-[2]C)	K^a	$\Delta G^\circ{}^b$ [kJ mol $^{-1}$]
323	0.735 ± 0.041	0.265 ± 0.041	5.86×10^{-5}	26.17
328	0.684 ± 0.033	0.316 ± 0.033	1.15×10^{-4}	24.74
333	0.635 ± 0.043	0.364 ± 0.043	2.03×10^{-4}	23.53
338	0.585 ± 0.040	0.415 ± 0.040	3.55×10^{-4}	22.32
343	0.529 ± 0.044	0.471 ± 0.044	6.35×10^{-4}	20.99
353	0.424 ± 0.046	0.576 ± 0.046	1.81×10^{-3}	18.53
358	0.382 ± 0.031	0.618 ± 0.031	2.75×10^{-3}	17.54

^a $\Delta K = \pm 10\%$, calculated for a 1.7 mM initial solution of **Zn-TK**. ^b $\Delta H^\circ = 106 \pm 7 \text{ kJ mol}^{-1}$; $\Delta S^\circ = 247 \pm 21 \text{ J mol}^{-1} \text{ K}^{-1}$.

landscape of the system **Zn-TK-Zn-[2]C**, however, should be different, according to the model^{19c} described by Revell and Williamson, namely the final product should be fairly more stable than the reactant species. The actual characteristics of **Zn-TK** conversion into **Zn-[2]C** are more complex than a model entailing only a single intermediate between the reactant(s) and product(s) because of the occurrence of a pool of intermediates that most probably encompass the rate-determining step of the process. The analysis performed on the data obtained from the samples kept in oil bath and affected by temperature instability gave $\Delta H^\circ = 197 \text{ kJ mol}^{-1}$, $\Delta S^\circ = 589 \text{ J mol}^{-1} \text{ K}^{-1}$. The operative approach leading to the results in Table 1 overestimates the stability of **Zn-TK** over **Zn-2[C]** and represents most likely only the pre-equilibrium step between **Zn-TK** and the intermediate pool of the conversion process. Nonetheless those apparent parameters measured under controlled temperature conditions convey information highlighting the thermal switch characteristics of the considered species that could be exploited within specific temperature intervals.

Effect of bromide ion

We recently reported the anion-assisted formation and anion binding properties of **Zn-TK** in aqueous solutions.¹⁵ We found that, in presence of tetrabutylammonium bromide, two CF_3COO^- counter-anions of **Zn-TK** are exchanged with two bromide anions that become firmly fixed within the central cavity of **Zn-TK** cavity by means of electrostatic and CH-anion interactions. At 298 K, the log of the global binding constant, β_2 , for the two bromides in D_2O is 6. In the present study, we found that **Zn-TK** is converted quantitatively to **Zn-[2]C** after 12 days in D_2O at 50 °C (Fig. S11b†). However, the conversion is inhibited if bromide is present, and the effect is more pronounced at lower temperature. For example, after 12 days at 50 °C, the relative abundance of **Zn-[2]C** reached only 27% if bromide was present in the reaction solution. These results demonstrate the inhibitory effect of bromide on the reaction and the enhanced thermal stability of the knot in the presence of bromide.

Transmetalation-coupled transformation of Cd-TK

By taking advantage of the labile nature of Cd(II) -based complexes,^{20a-c} we were recently able to achieve a Cd(II) to Zn(II) transmetalation^{20d} of our trefoil knot **Cd-TK**. The analogous transmetalation of our Cd(II) -based catenane, **Cd-[2]C**, has so far been unsuccessful, likely due to its greater compactness and consequent stability. In our efforts to develop a new and effective synthesis of metal-based [2]catenanes, we have adopted a synthetic strategy that combines transmetalation and topological transformation at elevated temperature. We anticipated that the greater stability of metal–nitrogen coordination bonds in zinc(II) complexes *versus* those in cadmium(II) complexes would favor the spontaneity of a **Cd-TK** to **Zn-TK** transmetalation at low temperature and that this step could be coupled to a subsequent topological transformation of **Zn-TK** to **Zn-[2]C** at high temperature. For qualitative comparison,

the thermal stability of **Cd-TK** was first examined by ^1H NMR spectroscopy at elevated temperature in aqueous solution. Upon heating a D_2O solution of 1.7 mM **Cd-TK**, new sets of highly symmetric peaks began to appear (Fig. S12†), just as they had when **Zn-TK** was heated. After more than 48 h, the proton signals of **Cd-TK** had disappeared completely and a new set of highly symmetric signals had appeared. The final product was also characterized by HRMS which showed two m/z maxima at 751.097 and 463.074, corresponding to $(\text{Cd-[2]C} \cdot 2 \text{CF}_3\text{COO}^-)^{2+}$ and $(\text{Cd-[2]C} \cdot \text{CF}_3\text{COO}^-)^{3+}$, respectively (Fig. 4a and S13†). Interestingly, we found that the conversion of **Cd-TK** to **Cd-[2]C** (Fig. 4a) proceeded faster than conversion of **Zn-TK** into **Zn-[2]C**. We attribute this difference to the weakness of Cd–N bonds relative to Zn–N bonds.

After this preliminary investigation of the thermal stability of **Cd-TK**, a 1.7 mM D_2O solution of **Cd-TK** was mixed with 20 equivalent of zinc(II) acetate and heated to 90 °C (Fig. 4b). The progress of the reaction was monitored at regular intervals by ^1H NMR spectroscopy and HRMS. New peaks that developed in the ^1H NMR spectra revealed that the lower symmetry of the **Cd-TK** complex was broken and that species of higher symmetry were forming. After 60 h, resonances of **Cd-TK** had disappeared completely and new sets of highly symmetric signals had appeared (Fig. S14†). HRMS showed two clear m/z maxima at 704.1375 and 431.7696 which correspond to $(\text{Zn-[2]C} \cdot 2 \text{CF}_3\text{COO}^-)^{2+}$ and $(\text{Zn-[2]C} \cdot \text{CF}_3\text{COO}^-)^{3+}$, respectively. These results strongly support the operation of a coupled transmetalation and thermally assisted conversion in the reaction of **Cd-TK** to **Zn-[2]C**. HRMS also identified a large pool of intermediates in this system (Fig. S15b†).

Transmetalation and conversion were also performed sequentially (Fig. 4c): a 1.7 mM solution of **Cd-TK** in D_2O was

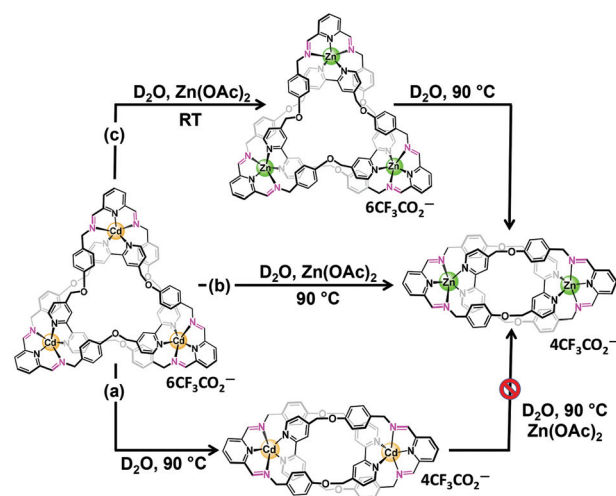


Fig. 4 (a) Transformation of **Cd-TK** into **Cd-[2]C** in D_2O at 90 °C. (b) Heat-induced transformation of **Cd-TK** into **Zn-[2]C** occurring in the presence of 20 equivalent of zinc acetate in aqueous solution at 90 °C; (c) *in situ* transmetalation of **Cd-TK** to **Zn-TK** in D_2O with 20 eq. of Zn(OAc)_2 at room temperature (RT), followed by heat-induced transformation of **Zn-TK** into **Zn-[2]C** at 90 °C; **Cd-[2]C** resisted transmetalation with zinc, as indicated by the red stop sign.

first transmetalated with 20 equivalents of $\text{Zn}(\text{OAc})_2$ at room temperature to form **Zn-TK**. The solution was then heated to 90 °C to form **Zn-[2]C**, which was identified by HRMS (Fig. S15†). The transmetalation of **Cd-[2]C** to **Zn-[2]** in the presence of 20 equivalents of $\text{Zn}(\text{OAc})_2$ was, however, unsuccessful. We attribute the failure of this reaction to the compactness and greater kinetic stability of the catenane structure.

Conclusions

In conclusion, we have achieved a thermally assisted conversion of a molecular knot, **Zn-TK**, into a molecular link, **Zn-[2]C** in D_2O . From the proton NMR studies, we found that the rate of the transformation increases with increasing temperature. Kinetic analysis by HRMS showed that the transformation involves a library of intermediates that form after the imine bonds of the trefoil knot are cleaved. In a separate set of experiments, we found that bromide ions inhibit the reaction by lodging within the central cavity of **Zn-TK**. The analogous conversion of a cadmium-based trefoil knot, **Cd-TK**, to the corresponding [2]catenane, **Cd-[2]C** was also accomplished and occurred faster because of the weaker metal–nitrogen coordination bonds in the cadmium complexes. The conversion of **Cd-TK** to **Zn-[2]C** was effected as well. This process involves transmetalation followed by heat-induced topological transformation. It could be performed in one or two procedural steps: either at 90 °C in the presence of $\text{Zn}(\text{OAc})_2$ or by transmetalation at room temperature followed by heat-induced topological transformation at 90 °C.

Several interconversions between topologically non-trivial metal–ligand complexes have been described previously.¹⁷ Equilibria between gold-containing [2]catenanes and Solomon links,^{17a} as well as between Solomon links and Borromean rings,^{17b} have been reported. Clever and coworkers have recently discovered an anion-induced rearrangement of a triply-interlocked cage to a [3]catenane.^{17c} In these three systems, equilibria between the complexes were established by mixing ligands and metal templates, and products were individually isolated, if possible. The Murkerjee group, on the other hand, have described the isolation and characterization of a triply interlocked cage, which was subsequently dimerized.^{17d} The dimer was also fully characterized and could be converted to starting material thermally. In our system, the forward transformation involves unraveling of the knots followed by reconfiguration to form the [2]catenanes. The [2]catenanes are composed of fewer units and are therefore surely entropically driven.^{14,15} However, we've found that bromide ion tips the thermodynamic balance enthalpically toward the knots and may provide a means for running the reaction in reverse.

Conflicts of interest

There are no conflicts to declare.

Acknowledgements

The research described here was sponsored by New York University Abu Dhabi, in the UAE. T. P., G. E and A. T. thank NYUAD for its generous support for the research program at NYUAD. We would like to acknowledge the Al Jalila Foundation (AJF201646) for funding this research work. The authors also thank the Core Technology Platforms at NYUAD. M. E. and L. C. thank the CNRS and the University of Strasbourg.

Notes and references

- (a) R. Chakrabarty, P. S. Mukherjee and P. J. Stang, *Chem. Rev.*, 2011, **111**, 6810–6918; (b) M. Fujita, M. Tominaga, A. Hori and B. Therrien, *Acc. Chem. Res.*, 2005, **38**, 369–378; (c) K. Harris, D. Fujita and M. Fujita, *Chem. Commun.*, 2013, **49**, 6703–6712; (d) D. L. Caulder and K. N. Raymond, *J. Chem. Soc., Dalton Trans.*, 1999, 1185–1200; (e) T. K. Ronson, Z. Salvatore, S. P. Black and J. R. Nitschke, *Chem. Commun.*, 2013, **49**, 2476–2490; (f) A. M. Castilla, W. J. Ramsay and J. R. Nitschke, *Acc. Chem. Res.*, 2014, **47**, 2063–2073; (g) C. Piguet, G. Bernardinelli and G. Hopfgartner, *Chem. Rev.*, 1997, **97**, 2005–2062; (h) C. G. Oliveri, P. A. Ulmann, M. J. Wiester and C. A. Mirkin, *Acc. Chem. Res.*, 2008, **41**, 1618–1629; (i) F. A. Cotton, C. Lin and C. A. Murillo, *Acc. Chem. Res.*, 2001, **34**, 759–771; (j) V. G. Machado, P. N. Baxter and J. M. Lehn, *J. Braz. Chem. Soc.*, 2001, **12**, 431–462; (k) R. J. Puddephatt, *Chem. Soc. Rev.*, 2008, **37**, 2012–2027.
- (a) W. Wang, Y.-X. Wang and H.-B. Yang, *Chem. Soc. Rev.*, 2016, **45**, 2656–2693; (b) A. J. McConnell, C. S. Wood, P. P. Neelakandan and J. R. Nitschke, *Chem. Rev.*, 2015, **115**, 7729–7793.
- R. A. Bilbeisi, J.-C. Olsen, L. J. Charbonnière and A. Trabolsi, *Inorg. Chim. Acta*, 2014, **417**, 79–108.
- T. Weilandt, R. W. Troff, H. Saxell, K. Rissanen and C. A. Schalley, *Inorg. Chem.*, 2008, **47**, 7588–7598.
- T. Yamamoto, A. M. Arif and P. J. Stang, *J. Am. Chem. Soc.*, 2003, **125**, 12309–12317.
- M. Kieffer, B. S. Pilgrim, T. K. Ronson, D. A. Roberts and M. Aleksanyan, *J. Am. Chem. Soc.*, 2016, **138**, 6813–6821.
- A.-M. Stadler, J. Ramirez, J.-M. Lehn and B. Vincent, *Chem. Sci.*, 2016, **7**, 3689–3693.
- X. Lu, X. Li, K. Guo, T.-Z. Xie, C. N. Moorefield, C. Wesdemiotis and G. R. Newkome, *J. Am. Chem. Soc.*, 2014, **136**, 18149–18155.
- R. Custelcean, *Chem. Soc. Rev.*, 2014, **43**, 1813–1824.
- O. Gidron, M. Jirasek, N. Trapp, M.-O. Ebert, X. Zhang and F. Diederich, *J. Am. Chem. Soc.*, 2015, **137**, 12502–12505.
- N. Kishi, M. Akita and M. Yoshizawa, *Angew. Chem., Int. Ed.*, 2014, **53**, 3604–3607.
- M. Han, Y. Luo, B. Damaschke, L. Gomez, X. Ribas, A. Jose, P. Peretzki, M. Seibt and G. H. Clever, *Angew. Chem., Int. Ed.*, 2016, **55**, 445–449.

- 13 B. Thomas, R. E. Powers, T. N. Parac, N. Tatjana and K. N. Raymond, *J. Am. Chem. Soc.*, 1999, **121**, 4200–4206.
- 14 T. Prakasam, M. Lusi, M. Elhabiri, C. Platas-Iglesias, J.-C. Olsen, Z. Asfari, S. Cianfèrani-Sanglier, F. Debaene, L. J. Charbonnière and A. Trabolsi, *Angew. Chem., Int. Ed.*, 2013, **52**, 9956–9960.
- 15 R. A. Bilbeisi, T. Prakasam, M. Lusi, R. El Khoury, C. Platas-Iglesias, L. J. Charbonnière, J.-C. Olsen, M. Elhabiri and A. Trabolsi, *Chem. Sci.*, 2016, **7**, 2524–2531.
- 16 Unless the number of counter anions have been made explicit, **TK** refers to a trefoil knot and six associated trifluoroacetates and **[2]C** refers to a **[2]**catenane and four associated CF_3COO^- .
- 17 (a) C. P. McArdle, M. C. Jennings, J. J. Vittal and R. J. Puddephatt, *Chem. – Eur. J.*, 2001, **7**, 3572–3583; (b) C. D. Pentecost, K. S. Chichak, A. J. Peters, G. W. V. Cave, S. J. Cantrill and J. F. Stoddart, *Angew. Chem., Int. Ed.*, 2007, **46**, 218–222; (c) R. Zhu, J. Lubben, B. Dittrich and G. H. Clever, *Angew. Chem., Int. Ed.*, 2015, **54**, 2796–2800; (d) D. Samanta and P. S. Mukherjee, *J. Am. Chem. Soc.*, 2014, **136**, 17006–17009.
- 18 (a) J. P. Sauvage, *Top. Curr. Chem.*, 2012, **323**, 107–126; (b) D. M. Walba, *Tetrahedron*, 1985, **41**, 3161–3212; (c) R. S. Forgan, J.-P. Sauvage and J. F. Stoddart, *Chem. Rev.*, 2011, **111**, 5434–5464.
- 19 (a) T. Weilandt, R. W. Troff, H. Saxell, K. Rissanen and C. A. Schalley, *Inorg. Chem.*, 2008, **47**, 7588–7598; (b) T. Yamamoto, A. M. Arif and P. J. Stang, *J. Am. Chem. Soc.*, 2003, **125**, 12309–12317; (c) L. E. Revell and B. E. Williamson, *J. Chem. Educ.*, 2013, **90**, 1024–1027.
- 20 (a) D. B. Berezin, O. V. Shukhto and N. V. Lazareva, *Russ. J. Inorg. Chem.*, 2012, **57**, 744–750; (b) S. V. Zvezdina, M. B. Berezin and B. D. Berezin, *Russ. J. Inorg. Chem.*, 2006, **51**, 112–117; (c) D. L. Rabenstein, G. Blakney and B. J. Fuhr, *Can. J. Chem.*, 1975, **53**, 787–791; (d) T. Prakasam, R. A. Bilbeisi, M. Lusi, J.-C. Olsen, C. Platas-Iglesias and A. Trabolsi, *Chem. Commun.*, 2016, **52**, 7398–7401.